EXPERIMENTAL STUDY ON QUALITY LOSS AND MICROSTRUCTURAL CHARACTERISTICS OF REINFORCED CONCRETE IN BRIDGE DECK PANELS AFTER SALT FREEZING

Xilong Zheng[1], Di Guan[2], Honglei Zhang[3]

1. *School of Civil and Architectural Engineering, Harbin University, No.109 Zhongxing Road, Harbin, Heilongjiang Province, China; sampson88@126.com*

2. *School of Civil and Architectural Engineering, Harbin University, No.109 Zhongxing Road, Harbin, Heilongjiang Province, China*

3. *Bridge Department, Beijing New Bridge Technology Development Co., LTD, No.8 Xitucheng Road, Beijing, China*

ABSTRACT

The reinforced concrete structure is the most widely used structural form today. In the western salt-alkali areas and in road and bridge projects in the northern regions where de-icing agents are applied, chloride ion intrusion into concrete leads to rebar depassivation and corrosion. With the occurrence and intensification of corrosion, the expansion of corrosion products leads to cracking or spalling of the concrete cover, resulting in durability damage to the reinforced concrete structure. Among all the components of the bridge, the bridge deck panels suffer the most severe and direct damage from salt freezing. Therefore, predicting the service life under salt freezing conditions is an urgent issue to address for the durability design, evaluation, and structural maintenance decision-making for reinforced concrete bridge deck panels. Concrete specimens in both water and salt solutions follow a four-stage pattern of deterioration. After 300 freeze-thaw cycles, the mass loss rates of specimens in water, NaCl solution, Solution A, and Solution B were 0.56%, 2.36%, 3.39%, and 3.71% respectively. Using Matlab analysis software, it was found that specimens in Solution B reached the failure limit first after 410 freeze-thaw cycles.

KEYWORDS

Freeze-thaw, Salt freezing, Reinforced concrete bridge deck panel, Quality loss, Microscopic

INTRODUCTION

The investigation conducted by relevant departments of the Ministry of Transportation on highway bridges in the high latitudes of the world revealed that the service life of urban transportation and road and bridge systems will be significantly shortened under the application of deicing agents in high latitude areas [1, 2]. The erosion and destruction of concrete by salt is the comprehensive result of physical and chemical effects. Although soluble inorganic salts such as NaCl and $CaCl_2$ scattered on the pavement can prevent icing, some studies have shown that salt will aggravate the surface erosion of concrete. The physical and chemical action and corrosion of snow melting agent are very strong, which will cause chronic damage to the bridge panel [3, 4].

In China, the old Beijing Xizhimen overpass was demolished and rebuilt due to durability problems after only 18 years of operation, and the Shenyang Wenhua Road overpass was cracked

----

and spalling seriously after 13 years of use due to steel corrosion [5]. The Harbin-Daqing Highway, after being in operation for only 5 years, experienced severe longitudinal cracking and spalling of the concrete [6]. It is reported that a large number of snow melting agents have been used abroad in the past few years, which has caused serious corrosion damage to buildings mainly dominated by Bridges, and huge economic losses [5]. Foreign investigations have shown that Bridges that use snowmelt agents show corrosion damage in about 15 years [6]. In the United States, a quarter of highway Bridges have been restricted due to corrosion of concrete and steel bars caused by snowmelt, of which 1% (about 5,000) are no longer open to traffic, and the maintenance cost alone is as high as $90 billion [7]. The UK has spent 6.2 billion pounds repairing Bridges damaged by corrosion caused by snowmelt [8]. The United States has done an experiment, the original design life of an overpass is 50 years, if the use of snow melt agent snow removal, the life of the overpass may drop to 20 years, or even 15 years, which seriously hindered traffic, damage public property, the harm cannot be ignored [9,10].

There is a lack of research in China and even in developed countries regarding the assessment of the harmful effects of de-icing agents on highways and bridges. There is also a lack of reasonable methods to evaluate the corrosiveness of de-icing agents, and no rational evaluation system has been established [11-13]. Therefore, conducting technical research on the erosion mechanism of de-icing agents on reinforced concrete bridge decks, the permeation pattern of chloride ions, and the impact of de-icing agents on their durability has become an urgent issue for highway authorities. The aim is to reduce the harm caused by de-icing agents to bridges and the environmental pollution they cause [14-16].

This project adopts the method of coupling chloride salt solution and freeze-thaw cycles to explore the distribution, migration, and microstructural evolution of chloride ions in reinforced concrete bridge decks. It reveals the impact of chloride ion diffusion on the bond stress of reinforced concrete and analyzes the collaborative performance of test beams in terms of concrete quality loss after salt freezing damage. The findings will provide a theoretical basis and technical support for design departments to carry out durability design of concrete bridge decks in cold regions, as well as for transportation management departments in terms of controlling the use of de-icing materials, evaluating their harmfulness to highways and bridges, and predicting their service life. This research is of significant theoretical and practical value, as it guarantees the long-term safe operation of infrastructure in China and promotes rapid and sustained economic development. It also helps reduce maintenance costs of highways, bridges, and other infrastructure, leading to important economic and social benefits.

DETERMINATION OF SURFACE DELAMINATION MORPHOLOGY AND MASS LOSS OF SPECIMENS AFTER SALT FREEZING

Test summary

The concrete mass loss rate reflects the degree of erosion of the concrete protective layer during salt freezing cycles and is an important factor affecting concrete durability. It can be used as an indicator to evaluate concrete durability. It is generally considered that when the concrete mass loss reaches 5%, it is considered as failure. Concrete salt freezing damage can be roughly divided into four stages: (1) Surface without obvious damage, with minor pitting erosion. (2) With increasing freeze-thaw cycles, the surface mortar begins to erode, resulting in small pits and grooves. (3) Severe erosion of the surface mortar, deeper and larger pits and grooves, exposure of fine aggregates, and slight erosion. (4) Severe erosion of fine aggregates, exposing coarse aggregates, and the concrete texture becomes porous.

1. Composition of the immersion solution for freeze-thaw specimens

There are four types of immersion solutions, including water, NaCl solution, a solution with a

----

mass ratio of NaCl: $MgCl_2$: $CaCl_2$=6:2:2, and a solution with a mass ratio of NaCl: $MgCl_2$: $CaCl_2$=6:3:1. The concentration of each solution is 3%. For convenience, the solution with a mass ratio of NaCl: $MgCl_2$: $CaCl_2$=6:2:2 is defined as solution A, and the solution with a mass ratio of NaCl: $MgCl_2$: $CaCl_2$=6:3:1 is defined as solution B.

2. Translate the raw materials such as cement and aggregates

The concrete mix ratio for casting the experimental beam is shown in Table 1. The cement used is Swan brand 42.5 ordinary Portland cement produced by Harbin Yatai Cement Co., Ltd. The coarse and fine aggregates are crushed stones with a maximum particle size of 16 mm and natural river sand with a fineness modulus of 2.5, respectively, in gradation Zone 11. The water-to-cement ratio of the concrete is 0.40, and the slump is 28 mm.

Tab. 1 - Concrete mix ratio and mechanical properties

W/C	Water （Kg）	Concrete （Kg）	Sand （Kg）	Stone （Kg）	28d Axial compressive strength f_{cu} （N/mm²）
0.4	166	415	600	1219	52.3

The reinforcement used Grade HRB335, and the mechanical properties of the reinforcement are shown in Table 2.

Tab. 2 - Mechanical properties of the reinforcement

Strength grade	Steel grade	Nominal diameter （mm）	Yield strength f_y （MPa）	Ultimate strength f_u （MPa）	Elongation δ_{10} （%）
HRB335	Ribbed steel bar	10	335	495	≥16

3. Sample preparation and grouping:

The experiment uses plain concrete specimens with dimensions of 100 mm×100 mm×400 mm, formed horizontally. A total of 12 specimens are prepared and divided into 4 groups. After being left to stand at room temperature for 24 hours, the specimens are demolded and numbered as follows: Group 1, numbered A13D~B33D; Group 2, numbered A41D~A43D; Group 3, numbered A11D~A31D; Group 4, numbered A12D~A32D. Different liquids are poured into each group during the freeze-thaw test, including water, NaCl solution, Solution A, and Solution B. To meet the requirements of the control study, 3 specimens without any damage treatment are prepared, making a total of 15 specimens. Freeze-thaw test was carried out in freeze-thaw chamber. Each cycle includes 2 hours of freezing and 2 hours of thawing. Freeze-thaw cycle diagram of concrete is shown in Figure 1.

Fig. 1 – Freeze-thaw cycle diagram of concrete

Experimental results and analysis

The erosion conditions of the specimens in water and Solution B are shown in Figure 2, from top to bottom, representing specimens subjected to 50, 150, and 250 freeze-thaw cycles respectively.
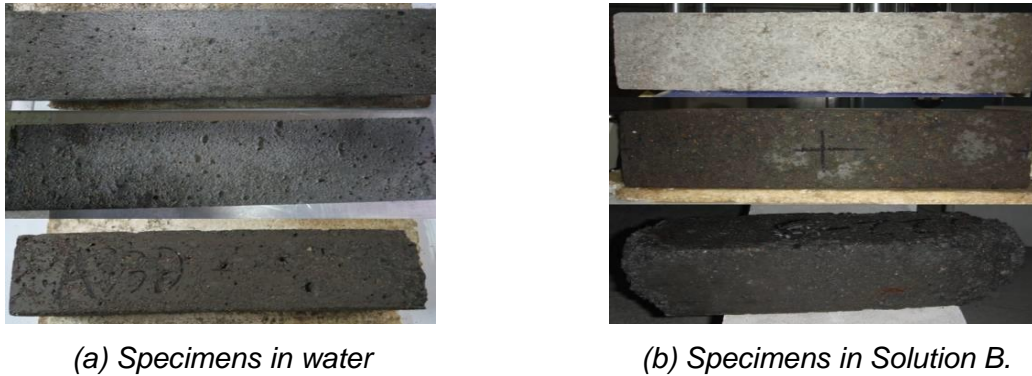

(a) Specimens in water

(b) Specimens in Solution B.

Fig. 2 – Visual changes of the specimen's external damage

The mass changes of the specimens during 300 freeze-thaw cycles in water and different solutions are shown in Figure 3.
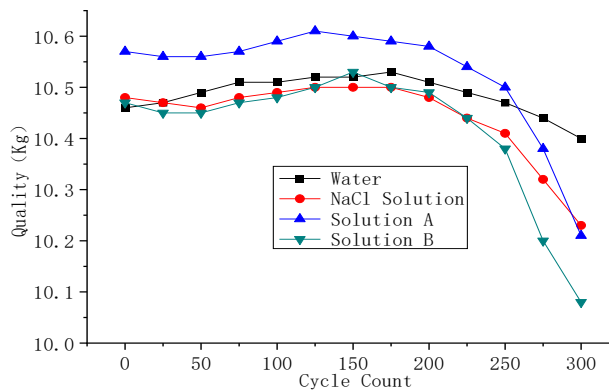

Fig. 3 – Graph of the mass changes of the specimens

Refer to Table 3 for the mass loss rate of the specimens as shown in Figure 4 - Figure 5.

Tab. 3 - Statistical table of specimen mass loss rate

Soaking liquid		Cycle count										
		0	25	50	75	100	125	150	200	225	275	300
Rate of quality loss%	Water	0	-0.14	-0.26	-0.49	-0.53	-0.60	-0.60	-0.46	-0.33	0.21	0.56
	NaCl solution	0	0.14	0.14	0.03	-0.08	-0.15	-0.17	0.01	0.34	1.56	2.35
	Solution A	0	0.05	0.04	-0.03	-0.19	-0.35	-0.28	-0.08	0.30	1.76	3.39
	Solution B	0	0.15	0.14	0.02	-0.14	-0.26	-0.54	-0.23	0.25	2.57	3.71

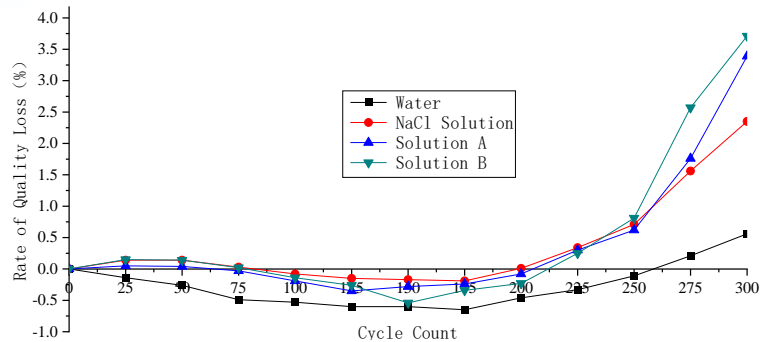

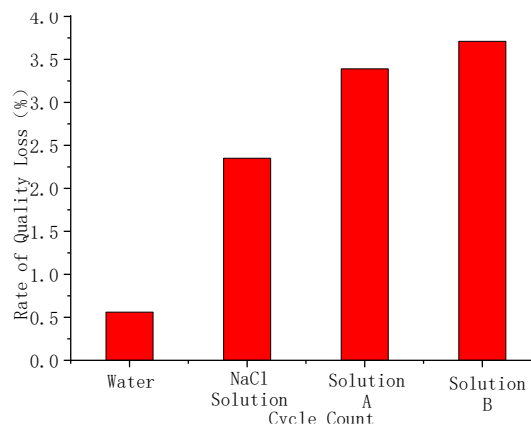*Fig. 4 – Graph of the specimen mass loss rate*

Fig. 5 – Mass loss rate of the specimens after 300 cycles

From Figure 3, it can be observed that the freeze-thaw damage test of the specimens in the salt solution follows the same four-stage failure mode. In Figure (b), the upper specimen is after 50 freeze-thaw cycles, with a smooth and flat surface. The middle specimen is after 150 cycles, and localized surface cracks and detachment of the surface mortar can be observed, but the damage is slight, with no exposed aggregates, and the local area remains smooth. The lower specimen is after 250 cycles, where the surface erosion is already severe, with pits and grooves throughout the specimen, significant loss of concrete mortar and fine aggregates, and even some detachment of coarse aggregates, exposing them. The cross-sectional area has reduced significantly, with the ends of the specimen resembling elliptical cones. When struck with a hard object, the surface feels loose, and materials may detach.

From Figure 4 and Figure 5, it can be seen that throughout the entire freeze-thaw cycle, the mass changes of the specimens do not continuously decrease. In the early stage (0-150 cycles) of the freeze-thaw test, there is a slight increase in mass for the specimens in water and different solutions, but the trend is relatively stable. In the middle and later stages, the mass loss of the specimens (especially in the different solutions) intensifies, and the mass loss curve becomes steeper. After 300 freeze-thaw cycles, the mass loss rates of the specimens in water, NaCl solution, Solution A, and Solution B are 0.56%, 2.36%, 3.39%, and 3.71% respectively.

This change in mass loss is caused by multiple factors, including temperature stress, osmotic pressure, and crystallization pressure. In the early stage, the intact concrete surface has a dense structure with low porosity and no significant cracks or defects. When the surface mortar undergoes freeze-thaw spalling, micro-pores and cracks are exposed, facilitating the penetration of ions. As the ions from the solution penetrate deep into the concrete, complex physicochemical reactions occur with the concrete materials, resulting in the formation of crystals and harmful substances. At this stage, the amount of reaction products slightly exceeds the amount of concrete spalling, leading to

----

a minor increase in the specimen's mass. As the mortar and fine aggregates further spall, the pore structure undergoes significant changes, which further facilitates the intrusion of ion media and intensifies the process of concrete spalling. The concrete spalling becomes much greater than the generation of physicochemical reaction products, resulting in a rapid increase in mass loss.

The experiment shows that chloride salt solution can significantly accelerate the freeze-thaw damage process of concrete structures. Taking 300 freeze-thaw cycles as an example, the mass loss rates of the specimens in NaCl solution, Solution A, and Solution B are 4.2, 6.0, and 6.5 times higher than that in water, respectively. Using Matlab analysis software fitting, it is found that the mass loss of specimens in Solution B will reach 5.02% (the limit specified in the standard is 5%) after 410 freeze-thaw cycles, reaching the failure limit first.

MICROSCOPIC ANALYSIS OF THE INTERFACE BETWEEN STEEL AND CONCRETE IN REINFORCED CONCRETE

Summary of the experiment

The core of modern materials science lies in the relationship between the microscopic structure inside the material and its properties. In the past, research on reinforced concrete focused on the study of macroscopic basic properties, including strength, load-bearing capacity, carbonation depth, and so on, with limited research conducted at the microscopic level. At the macroscopic scale, concrete materials are assumed to be uniform and isotropic, allowing various conventional tests to be conducted. However, this assumption does not hold at the microscopic level. Therefore, conducting only macroscopic research lacks accuracy and rigor. It is crucial and urgent to conduct in-depth research on the microscopic structure and mineral composition changes of reinforced concrete after salt freezing.

Scanning electron microscopy (SEM) can be used to observe the pore size distribution, coarse and fine aggregate morphology, hydration product structure, and the intrusion of harmful substances into the concrete and steel-concrete interface. This provides a microscopic basis for studying the salt freeze durability of reinforced concrete.

1. Testing apparatus

In this experiment, scanning electron microscopy (SEM) is employed to observe the microscopic morphology of the surface, interior, and steel-concrete interface of the reinforced concrete specimens. Additionally, elemental energy-dispersive spectroscopy (EDS) analysis is used to analyze the elemental content in various areas, studying the relationship between chloride (Cl-) content and changes in the concrete's microscopic structure.

In this experiment, the QUANTA200 scanning electron microscope (SEM) manufactured by Japan Electron Optics Co., Ltd. is used. The SEM operates at an accelerating voltage of 20 kV and has an instrument resolution of 3.5 nm. Elemental analysis is performed using the Oxford INCA energy-dispersive spectroscopy (EDS) analyzer. The scanning electron microscope (SEM) is shown in Figure 6.

Fig. 6 – Scanning electron microscope (SEM)

----

2. Sample preparation

In this experiment, specimens L20, L22, and L24 are used for the tensile test. After the completion of the tensile test, samples are taken from the surface of the specimen, 25 mm below the surface, and the steel-concrete interface. Three small samples are taken from each specimen, making a total of nine samples. The samples are dried to a constant weight and then undergo coating treatment before being observed under the QUANTA 200 scanning electron microscope.

All three specimens are subjected to salt freeze-thaw treatment using a solution of NaCl: $MgCl_2$: $CaCl_2$ in a ratio of 6:3:1. The number of freeze-thaw cycles for each specimen is 50, 100, and 150 respectively.

Experimental Results and Analysis

(1) Electron microscopy observation and elemental energy spectrum analysis of specimen L20 SEM images of the microstructure of concrete samples from specimen L20 are shown in Figure 7, and elemental energy spectrum analysis is presented in Figure 8 - Figure 10.
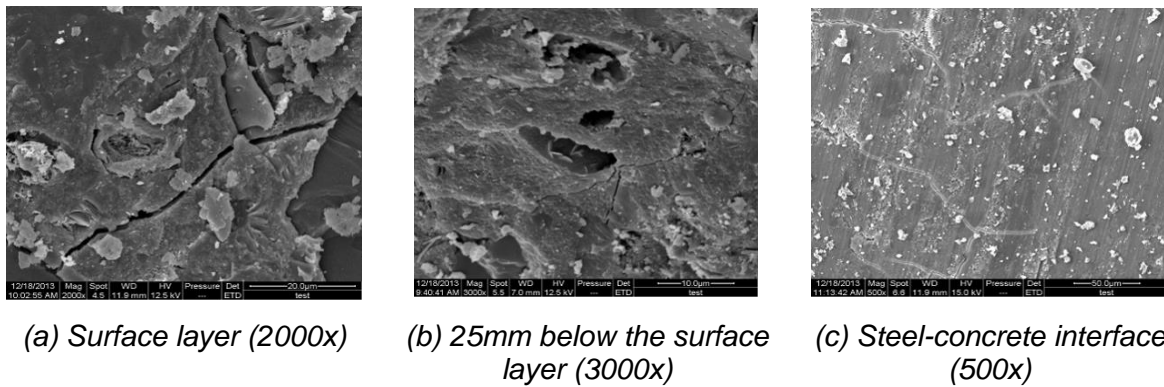

| (a) Surface layer (2000x) | (b) 25mm below the surface layer (3000x) | (c) Steel-concrete interface (500x) |

Fig. 7 – SEM images of microstructure of L20 specimen

Element	Wt%	At%
ClK	14.47	27.86
OK	20.70	29.91
NaK	00.54	00.54
MgK	04.20	03.99
AlK	03.51	03.00
SiK	20.49	16.87
KK	01.75	01.04
CaK	15.71	09.06
FeK	18.63	07.72
Matrix	Correction	ZAF
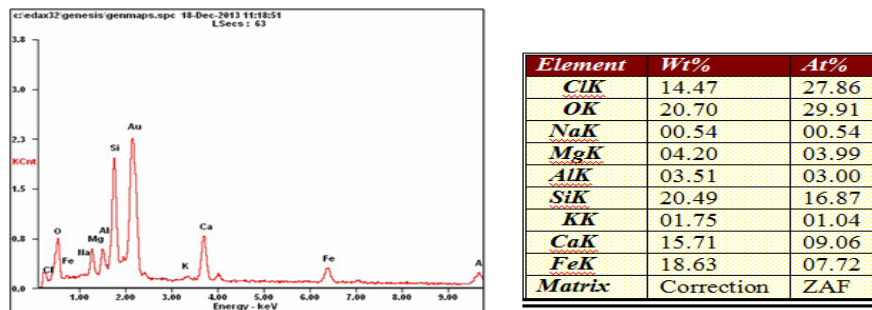
Fig. 8 – Energy-dispersive X-ray spectroscopy (EDS) analysis of surface elements of L20 specimen

----
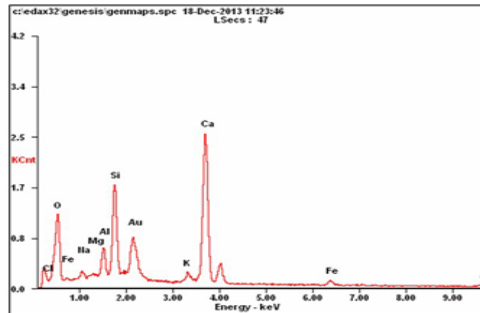
Element	Wt%	At%
ClK	09.92	18.64
OK	31.71	44.75
NaK	01.22	01.19
MgK	00.47	00.43
AlK	03.29	02.75
SiK	11.45	09.21
KK	02.01	01.16
CaK	35.98	20.27
FeK	03.96	01.60
Matrix	Correction	ZAF

Fig. 9– Energy-dispersive X-ray spectroscopy (EDS) analysis of elements at a distance of 25mm from the surface of L20 specimen
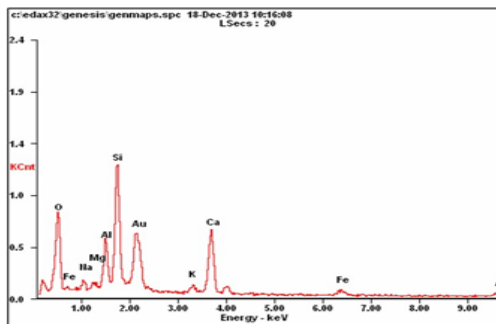
Element	Wt%	At%
OK	37.40	55.41
NaK	02.02	02.08
MgK	00.92	00.89
AlK	07.02	06.17
SiK	21.76	18.36
KK	02.44	01.48
CaK	21.14	12.50
FeK	07.31	03.10
Matrix	Correction	ZAF

Fig. 10 – Energy-dispersive X-ray spectroscopy (EDS) analysis of elements at the steel-concrete interface of L20 specimen

From the SEM images, it can be observed that cracks have occurred in the concrete at three different depths. Among them, the concrete cracks at the steel-concrete interface are narrow and short, mainly formed due to concrete shrinkage, and their development is limited as the internal temperature stress has little effect on them during freeze-thaw cycles. On the surface, there is a long crack in the concrete with a wider width. This crack is caused by significant strains due to temperature stress, resulting in severe damage. The concrete at a distance of 25 mm from the surface exhibits a level of damage between the two cases, with the cracks developing at the interplay of concrete shrinkage and temperature stress and showing some degree of progression.

After freeze-thaw cycles, the surface concrete becomes more porous and its permeability significantly decreases. There is also a certain development in the pore structure, and noticeable chloride salt products can be found on the surface. At a distance of 25 mm from the surface, no significant chloride salt products are detected, and the structure is relatively compact. The concrete at the steel-concrete interface appears relatively smooth and dense, exhibiting good overall integrity and resistance to permeability.

From the energy-dispersive X-ray spectroscopy (EDS) analysis, it can be observed that the distribution of Cl- varies significantly among different depths. The surface concrete has the highest content, with a mass percentage of up to 14.47% and a molar percentage of 27.86%. The concrete at a distance of 25 mm from the surface comes next, with a mass percentage of 9.92% and a molar percentage of 18.64%. No presence of Cl- is detected at the steel-concrete interface, indicating that after 50 freeze-thaw cycles, Cl- failed to effectively penetrate to the steel-concrete interface. The concrete at the steel-concrete interface is only subjected to temperature stress and has not been corroded by chloride salt media.

(2) Electron microscopy observation and elemental energy-dispersive X-ray spectroscopy (EDS) analysis of L22 specimen

Article no. 25

THE CIVIL ENGINEERING JOURNAL 3-2024

The microstructure SEM images of the concrete specimens of L22 are shown in Figure 11, and the elemental energy-dispersive X-ray spectroscopy (EDS) analyses are shown in Figure 12 - Figure 14.
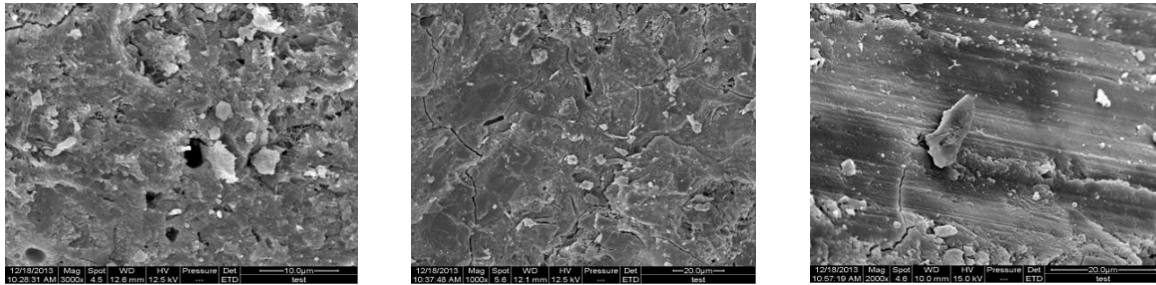

| (a) Surface layer (3000x) | (b) 25mm below the surface layer (1000x) | (c) Steel-concrete interface (2000x) |

Fig. 11 – SEM images of the microstructure of the L22 specimen
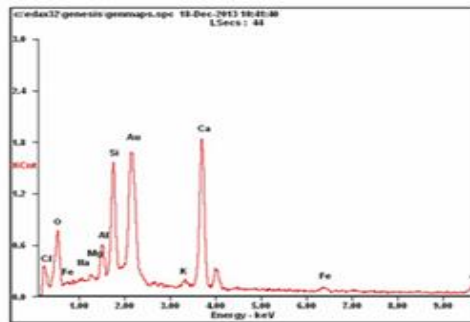
Element	Wt%	At%
ClK	15.23	29.46
OK	25.54	34.22
NaK	00.55	00.62
MgK	00.62	00.66
AlK	04.22	04.04
SiK	16.70	10.36
KK	01.70	01.12
CaK	31.15	17.52
FeK	04.28	01.98
Matrix	Correction	ZAF

Fig. 12 – Elemental energy-dispersive X-ray spectroscopy (EDS) analysis of the surface layer of the L22 specimen
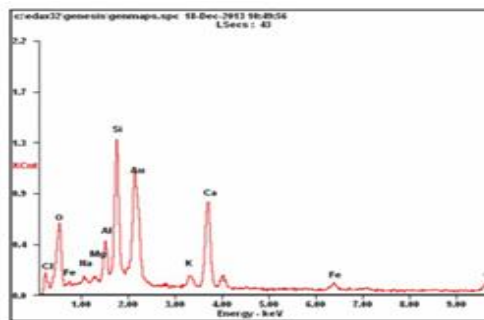
Element	Wt%	At%
ClK	10.52	20.01
OK	24.24	37.59
NaK	01.41	01.53
MgK	00.60	00.62
AlK	05.05	04.70
SiK	19.55	15.27
KK	03.74	02.40
CaK	27.46	14.53
FeK	07.44	03.34
Matrix	Correction	ZAF

Fig. 13 – Elemental energy-dispersive X-ray spectroscopy (EDS) analysis of the L22 specimen at a distance of 25mm from the surface layer

----

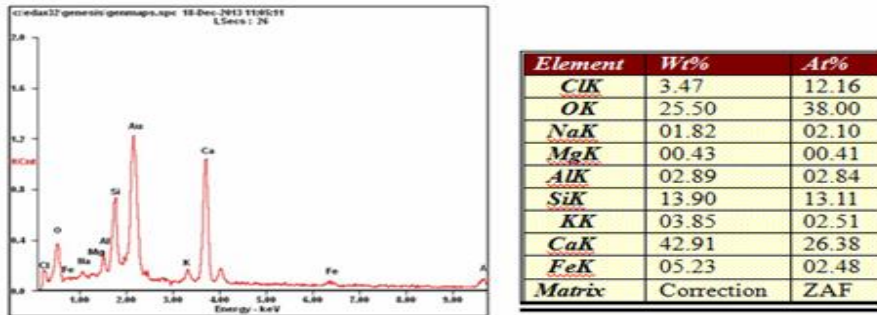| Element	Wt%	At%
ClK	3.47	12.16
OK	25.50	38.00
NaK	01.82	02.10
MgK	00.43	00.41
AlK	02.89	02.84
SiK	13.90	13.11
KK	03.85	02.51
CaK	42.91	26.38
FeK	05.23	02.48
Matrix	Correction	ZAF

Fig. 14 – Elemental energy-dispersive X-ray spectroscopy (EDS)
analysis of the steel-concrete interface of the L22 specimen

Based on the SEM images, it can be observed that cracks have developed in the concrete at different depths. The cracks at the steel-concrete interface are narrower, shorter, and more sporadic. They are mainly caused by concrete shrinkage, and the influence of internal temperature stress during freeze-thaw cycles is relatively minor. Therefore, the crack propagation is slow. The concrete at the surface layer exhibits a prominent crack with a wider width. This crack is a result of significant strain caused by temperature stress, leading to severe damage. The concrete at a distance of 25 mm from the surface layer shows intermediate levels of damage. Cracks have formed due to the combined effects of concrete shrinkage and temperature stress, with some degree of propagation.

After freeze-thaw cycles, the surface layer of the concrete becomes more porous, resulting in a significant decrease in permeability. The pore structure also develops to a certain extent, with numerous and larger-sized pores. There are visible chloride salt deposits on the surface. At a distance of 25 mm from the surface layer, a small amount of chloride salt deposits can be found, and the structure is relatively denser. The concrete at the steel-concrete interface is relatively smooth and compact, exhibiting overall integrity and good resistance to permeability.

The distribution of Cl- in different depths can be observed from the energy-dispersive X-ray spectroscopy analysis. The surface layer of the concrete has the highest concentration, with a mass percentage of 15.23% and a molar percentage of 29.46%. The Cl- content is lower at a depth of 25 mm from the surface layer, with a mass percentage of 10.52% and a molar percentage of 20.01%. The Cl- content is the lowest at the steel-concrete interface, with a mass percentage of 3.47% and a molar percentage of 12.16%, exceeding the critical value for inducing reinforcement corrosion. This indicates that Cl- has only penetrated to the steel-concrete interface after 100 freeze-thaw cycles, where the concrete is mainly affected by temperature stress and less influenced by chloride salt corrosion.

(3)   Electron microscopy observation and elemental energy-dispersive X-ray spectroscopy analysis of the L24 specimen

SEM images of the microstructures of concrete specimens for L24 specimen are shown in Figure 15, while the elemental energy-dispersive X-ray spectroscopy analyses are shown in Figure 16 - Figure 18.

Article no. 25

THE CIVIL ENGINEERING JOURNAL 3-2024
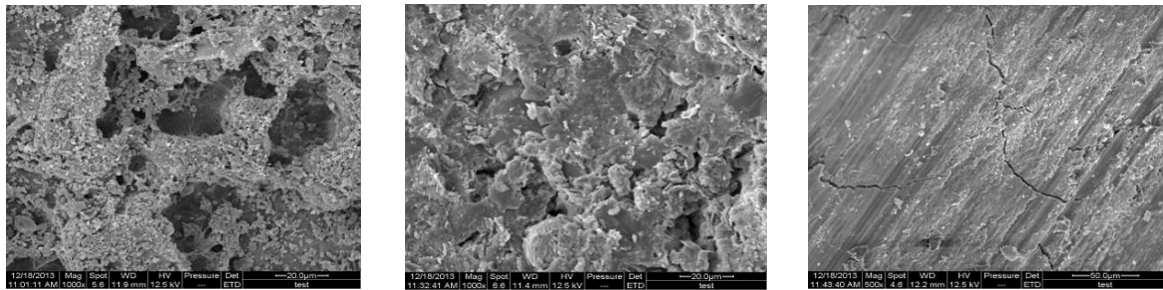
| (a) Surface layer (1000x) | (b) 25mm below the surface layer (1000x) | (c) Steel-concrete interface (500x) |

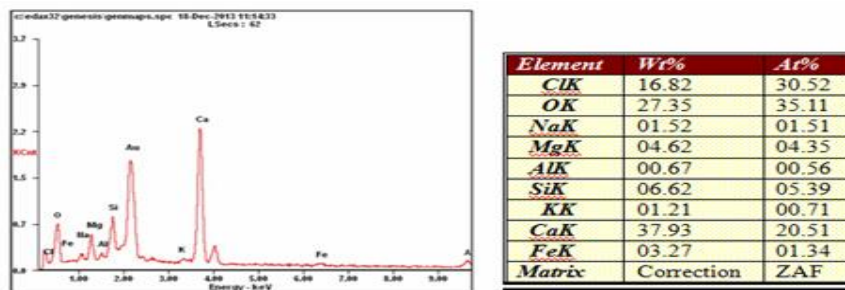*Fig. 15 – SEM images of the microstructure of the L24 specimen*

Element	Wt%	At%
ClK	16.82	30.52
OK	27.35	35.11
NaK	01.52	01.51
MgK	04.62	04.35
AlK	00.67	00.56
SiK	06.62	05.39
KK	01.21	00.71
CaK	37.93	20.51
FeK	03.27	01.34
Matrix	Correction	ZAF

Fig. 16 – Elemental energy-dispersive X-ray spectroscopy analysis of the surface layer of the L24 specimen

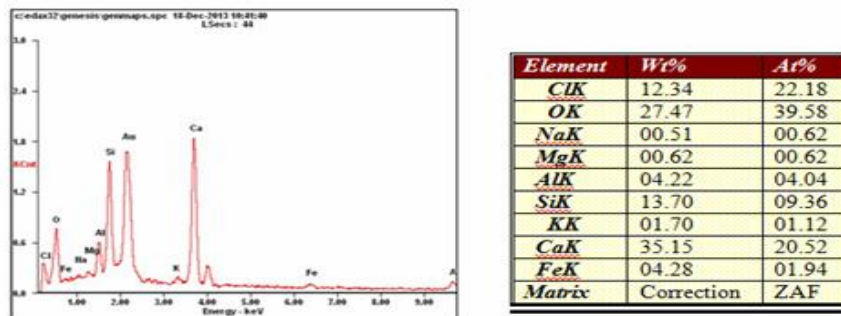| Element	Wt%	At%
ClK	12.34	22.18
OK	27.47	39.58
NaK	00.51	00.62
MgK	00.62	00.62
AlK	04.22	04.04
SiK	13.70	09.36
KK	01.70	01.12
CaK	35.15	20.52
FeK	04.28	01.94
Matrix	Correction	ZAF

Fig. 17 – Elemental energy-dispersive X-ray spectroscopy analysis of the L24 specimen at a distance of 25mm from the surface layer

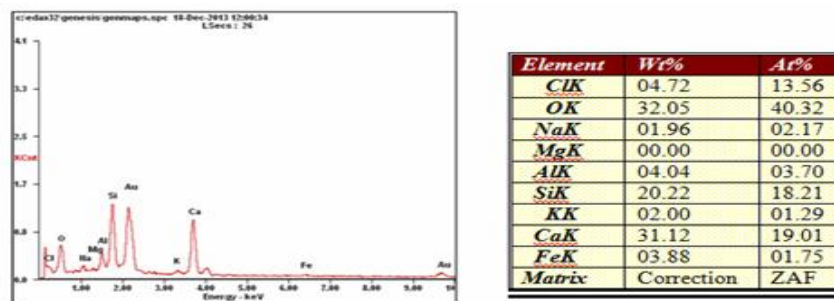| Element	Wt%	At%
ClK	04.72	13.56
OK	32.05	40.32
NaK	01.96	02.17
MgK	00.00	00.00
AlK	04.04	03.70
SiK	20.22	18.21
KK	02.00	01.29
CaK	31.12	19.01
FeK	03.88	01.75
Matrix	Correction	ZAF

Fig. 18 – Elemental energy-dispersive X-ray spectroscopy analysis at the steel-concrete interface of the L24 specimen

According to the SEM images, it can be observed that under the combined effects of concrete

----

shrinkage, temperature stress, and chloride ion erosion, the surface morphology of the concrete exhibits a honeycomb-like appearance, with severe loose, porous, and fragmented characteristics. The impermeability can be considered negligible as the surface is heavily covered with chloride salt deposits, indicating the loss of its protective structural function. The concrete cracks at the steel-concrete interface have significantly developed in width compared to 50 and 100 cycles of freeze-thaw cycles, transitioning from fine mesh-like cracks to coarse, deep-through cracks. No cracks were observed at a distance of 25 mm from the surface, but the concrete still exhibited severe loose, porous, and fragmented characteristics, leading to a significant reduction in impermeability.

From the energy-dispersive X-ray spectroscopy analysis, it can be observed that the content of Cl- increases significantly in different depth layers. The surface layer of the concrete has the highest content, with a mass fraction of up to 16.82% and a molar percentage of 30.52%. The content of Cl- at a distance of 25 mm from the surface is the second highest, with a mass fraction of 12.34% and a molar percentage of 22.18%. The Cl- content at the steel-concrete interface is the lowest, with a mass fraction of 4.72% and a molar percentage of 13.56%, exceeding the critical value for inducing steel corrosion. This indicates that after 100 cycles of freeze-thaw, Cl- has just penetrated the steel-concrete interface, where the concrete is primarily affected by temperature stress and has a lesser influence from chloride salt erosion.

Through comparison, the degree of concrete damage at the same location increases with the number of freeze-thaw cycles. After 50 cycles, the concrete damage is minimal, with only noticeable cracks on the surface layer. The development of concrete porosity is slow, and the texture is relatively compact. No significant chloride salt erosion is observed in the core region of the concrete. After 100 cycles, the concrete damage intensifies, with significant increases in the width and length of cracks in various areas. The concrete exhibits severe deterioration, reduced overall integrity, and decreased impermeability. The presence of chloride elements is detected in the core region of the concrete. After 150 cycles, the concrete damage in all areas becomes highly apparent. The protective function of the surface layer concrete is largely lost, and the Cl- content in the core region far exceeds the critical value for steel corrosion.

Based on the SEM images and energy-dispersive X-ray spectroscopy analysis at different freeze-thaw cycles and depths, it can be concluded that the penetration of chloride ions in concrete follows Fick's second law, with the ion permeation from the surface to the interior gradually decreasing and the erosion damage of the concrete diminishing. The damage to the steel-reinforced concrete occurs initially at the surface. Under the influence of multiple factors such as chloride salt and freeze-thaw, the chloride salt medium in the solution infiltrates into the concrete's interior through micro-cracks in the surface, filling the pore structure during crystallization. This induces pore structure expansion under the dual action of water freezing and expansion, damaging the microstructure of the concrete and further allowing the intrusion of chloride salt medium. The development of micro-cracks is caused by internal stresses resulting from salt crystallization, while the development of the pore structure and the formation of honeycomb morphology are the combined effects of chemical reactions with chloride salt medium and freeze-thaw actions.

CONCLUSION

The erosion and mass loss of various specimens after freeze-thaw cycles in water and different solutions were studied, and the variation patterns of mass loss rate under different freeze-thaw cycles and environments were analyzed. Through scanning electron microscopy (SEM) experiments, the morphology of hydrates, changes in micro-pore structure, and crack development in concrete at different depths after 50, 100, and 150 freeze-thaw cycles in Solution B were observed. Combined with energy-dispersive X-ray spectroscopy analysis, the permeation and distribution patterns of chloride ions were investigated. The following conclusions were primarily drawn:

(1) Concrete specimens in both water and salt solutions follow a four-stage pattern of

----

deterioration. However, under the combined effects of temperature stress and osmotic pressure, the mass of the specimens does not continuously decrease but rather exhibits a trend of slight increase in the early stages followed by a sharp decrease in the later stages. Furthermore, chloride ions can accelerate the freeze-thaw damage of concrete, with a higher concentration of chloride ions resulting in more pronounced deterioration. After 300 freeze-thaw cycles, the mass loss rates of specimens in water, NaCl solution, Solution A, and Solution B were 0.56%, 2.36%, 3.39%, and 3.71% respectively.

(2) From the SEM images, it can be observed that the concrete specimens exhibit different morphologies at different stages of deterioration. Initially, the surface appears dense and smooth, then it gradually develops spalling, roughness, and discolored areas. Eventually, a significant loss of mortar, fine aggregates, and coarse aggregates occurs. The crack pattern also transitions from fine interconnected cracks to larger and deeper penetrating cracks. The development of cracks accelerates the erosion of the concrete, which explains the phenomenon of a sharp increase in the mass loss rate of the specimens in the later stages of freeze-thaw cycles.

(3) From the energy-dispersive X-ray spectroscopy analysis, it can be observed that the penetration of chloride ions in concrete follows the basic principles of Fick's second law. After 50 freeze-thaw cycles, chloride ions have not yet penetrated the steel-concrete interface. However, after 100 freeze-thaw cycles, the presence of chloride ions is detected at the steel-concrete interface, and their concentration exceeds the regulatory requirements, which can lead to corrosion of the reinforcing steel and a decrease in bond stress. After 150 freeze-thaw cycles, the chloride ion content at the steel-concrete interface far exceeds the critical threshold for inducing reinforcement corrosion. Additionally, severe concrete spalling occurs at the surface, causing a significant loss of the concrete's protective function.

(4) This corrosive effect not only affects the aesthetic and structural integrity of the concrete, but also reduces its service life and safety. Therefore, when using deicing salt, it is necessary to weigh its advantages and disadvantages and take appropriate protective measures, such as using an isolated coating system to isolate the direct contact between deicing salt and concrete to reduce damage.

ACKNOWLEDGEMENTS

REFERENCES

[1] Liu D, Tu Y, Sas G, 2021. Freeze-thaw damage evaluation and model creation for concrete exposed to freeze–thaw cycles at early-age. Construction and Building Materials, vol. 312, 125352. https://doi.org/ 10.1016/j.conbuildmat.2021.125352

[2] Polat R, Demirboğa R, Karakoç M B, 2010. The influence of lightweight aggregate on the physico-mechanical properties of concrete exposed to freeze–thaw cycles. Cold Regions Science and Technology, vol. 60, no. 1, p. 51-56. https://doi.org/ 10.1016/j.coldregions.2009.08.010

[3] Li W, Pour-Ghaz M, Castro J, 2012. Water absorption and critical degree of saturation relating to freeze-thaw damage in concrete pavement joints. Journal of Materials in Civil Engineering, vol. 24, no. 3, p. 299-307. https://doi.org/ 10.1016/j.coldregions.2009.08.010

[4] Subramaniam K V, Ali-Ahmad M, Ghosn M, 2018. Freeze–thaw degradation of FRP–concrete interface: Impact on cohesive fracture response. Engineering Fracture Mechanics, vol. 75, no. 13, p. 3924-3940. https://doi.org/ 10.1016/j.engfracmech.2007.12.016

[5] Yun Y, Wu Y F, 2011. Durability of CFRP–concrete joints under freeze–thaw cycling. Cold Regions Science and Technology, vol. 65, no. 3, p. 401-412. https://doi.org/ 10.1016/j.coldregions.2010.11.008

----

[6] Peng R, Qiu W, Teng F, 2020. Three-dimensional meso-numerical simulation of heterogeneous concrete under freeze-thaw. Construction and Building Materials, vol. 250, p. 118573. https://doi.org/ 10.1016/j.conbuildmat.2020.118573

[7] Cai L, Wang H, Fu Y, 2013. Freeze–thaw resistance of alkali–slag concrete based on response surface methodology. Construction and Building Materials, vol. 49, p. 70-76. https://doi.org/ 10.1016/j.conbuildmat.2013.07.045

[8] Wang Z, Zeng Q, Wu Y, 2014. Relative humidity and deterioration of concrete under freeze–thaw load. Construction and Building Materials, vol. 62, p.18-27. https://doi.org/ 10.1016/j.conbuildmat.2014.03.027

[9] Xu S, Li A, Ji Z, 2016. Seismic performance of reinforced concrete columns after freeze–thaw cycles. Construction and Building Materials, vol. 102, p. 861-871. https://doi.org/ 10.1016/j.conbuildmat.2015.10.168

[10] Santana Rangel C, Amario M, Pepe M, 2020. Durability of structural recycled aggregate concrete subjected to Freeze-Thaw cycles. Sustainability, vol. 12, no. 16, p. 6475. https://doi.org/ 10.3390/su12166475

[11] Guo J, Sun W, Xu Y, 2022. Damage mechanism and modeling of concrete in freeze–thaw cycles: a review[J]. Buildings, vol. 12, no. 9, p. 1317. https://doi.org/ 10.3390/buildings12091317

[12] Liu Y, Chen Y F, Wang W, 2016. Bond performance of thermal insulation concrete under freeze–thaw cycles. Construction and Building Materials, vol. 104, p. 116-125. https://doi.org/ 10.1016/j.conbuildmat.2015.12.040

[13] Yu H, Ma H, Yan K, 2017. An equation for determining freeze-thaw fatigue damage in concrete and a model for predicting the service life. Construction and building materials, vol. 137, p. 104-116. https://doi.org/ 10.1016/j.conbuildmat.2017.01.042

[14] Alsaif A, Bernal S A, Guadagnini M, 2019. Freeze-thaw resistance of steel fibre reinforced rubberised concrete. Construction and Building Materials, vol. 195, p. 450-458. https://doi.org/ 10.1016/j.conbuildmat.2018.11.103

[15] Zhang K, Zhou J, Yin Z, 2021. Experimental study on mechanical properties and pore structure deterioration of concrete under freeze–thaw cycles. Materials, vol. 14, no. 21,p. 6568. https://doi.org/ 10.3390/ma14216568

[16] Bao J, Xue S, Zhang P, 2021. Coupled effects of sustained compressive loading and freeze–thaw cycles on water penetration into concrete. Structural Concrete, vol. 22, p. E944-E954. https://doi.org/ 10.1002/suco.201900200